JOURNAL OF MATERIALS SCIENCE 26 (1991) 2879–2886

# Precipitation hardening and recrystallization in Cu–4% to 7% Ni–3% Al alloys

YOUNG-RAE CHO, YOUNG-HO KIM, TAEK DONG LEE
*Division of Metals, Korea Institute of Science and Technology, PO Box 131, Cheongryang, Seoul, Korea*

The effects of microstructure on mechanical properties in three cold-worked Cu–4% to 7% Ni–3% Al alloys have been investigated by changing ageing time at 500 °C. Hardness and strength in the Cu–7% Ni–3% Al and Cu–5.5% Ni–3% Al alloys increase with ageing time and have maximum values at an ageing time of $10^3$–$10^4$ s at 500 °C, then decrease. During ageing of Cu–7% Ni–3% Al at 500 °C, the coherent $Ni_3Al$ phase was first precipitated out and later incoherent NiAl phase was formed. $Ni_3Al$ formed during the initial stage of ageing is likely to be a transient phase. The increases in hardness and strength are due to the precipitation of coherent $Ni_3Al$ phase. Coherent $Ni_3Al$ particles are effective in increasing the strength and retarding the recrystallization process. On the other hand, the hardness and strength in the Cu–4% Ni–3% Al alloy gradually declined with ageing time. Only incoherent NiAl phase was formed during ageing at 500 °C. Decreases in hardness and strength in the Cu–4% Ni–3% Al alloy are attributed to softening during recovery and recrystallization, because incoherent NiAl particles have an insufficient effect to increase the strength.

## 1. Introduction

Precipitation hardening in Cu-base alloys has been widely used to increase the strength. Several examples of precipitation hardening are shown in Cu alloys containing small amounts of alloying elements such as Be [1, 2], Ti [3], Al [4]. In these alloy systems, solute atoms react with the Cu matrix to form the precipitates which cause hardening.

Precipitation hardening was also observed by adding small amounts of Ni and Al to the Cu matrix [5, 6]. This case is different from the above alloys in that Ni and Al combine together to form precipitates where precipitate-forming elements are in limited supply and Cu serves as a simple matrix. A few papers have been published concerning the precipitation hardening in Cu–Ni–Al alloys. Leo and co-workers studied the precipitation phenomena in Cu–Ni–Al alloys [5, 6]. They observed that $Ni_3Al$ and NiAl particles were precipitated during ageing and suggested that coherent $Ni_3Al$ precipitates caused the hardness increase. Tsuda *et al.* [7] also investigated the deformation behaviour in aged Cu–5 at % Ni–2.5 at % Al and proposed that the strengthening mechanism resulted from the interaction of dislocations with the spherical particles of $Ni_3Al$.

In the present work, the precipitation hardening of the three cold-worked Cu–Ni–Al alloys, with a Ni content of 4–7 wt % and a fixed Al content of 3 wt %. In addition to ageing, cold working is also effective in increasing the strength [2, 4, 8]. Because cold working is usually introduced immediately after solution treatment, subsequent ageing yields recovery and recrystallization of the cold-worked structure as well as precipitation of secondary phase. The changes in mechanical strength during ageing in precipitation hardenable cold-worked Cu alloys should be discussed in terms of a process of microstructural change accompanying not only recovery and recrystallization, but also precipitation.

We have characterized the microstructural changes in the cold-worked Cu alloys during the ageing and recrystallization process. The influence of microstructure on the mechanical properties has also been investigated. In particular, the role of $Ni_3Al$ and NiAl phases is addressed.

## 2. Experimental procedure

The Cu alloys used here were vacuum melted from high-purity metals. Their compositions are listed in Table I. Cast ingots were homogenized for 24 h at 800 °C under an argon atmosphere and then hot rolled to 1.8 mm thick sheets. These sheets were solution-treated for 30 min at 910 °C and cold rolled prior to ageing. The cold reduction ratio was 77%. The alloys were subsequently aged at 500 °C for 1–$10^5$ s. In one case, Cu–7Ni alloy was aged up to $2 \times 10^6$ s for X-ray diffraction study. Ageing was carried out in a salt bath of $NaNO_3$ and $KNO_3$ solution.

Microhardness measurements were performed using a Vickers hardness tester. The applied load was 300 g and an average value was obtained from ten different tests. Tensile testing was carried out at ambient temperature with standard flat tensile specimens. X-ray diffractometry and transmission electron microscopy (TEM) were used to identify the types of precipitates. Thin foils for TEM study were prepared by electropolishing in a solution of 6% $HNO_3$ and 94%

0022–2461/91 $03.00 + .12 

TABLE I Chemical compositions (wt %) of Cu–Ni–Al alloys

| | Expected composition | Analysed value | |
|---|---|---|---|
| | | Ni | Al |
| Cu–4Ni | Cu–4.0% Ni–3% Al | 4.03 | 2.92 |
| Cu–5.5Ni | Cu–5.5% Ni–3% Al | 5.52 | 2.91 |
| Cu–7Ni | Cu–7.0% Ni–3% Al | 6.97 | 2.91 |

ethyl alcohol. The temperature was kept below $-30\,^{\circ}C$ during electropolishing. TEM foils were characterized at 160 or 200 kV in a Jeol 200 CX microscope.

## 3. Results

### 3.1. Mechanical properties

Fig. 1 shows the variation of the microhardness with ageing time at 500 °C in the three cold-rolled Cu alloys. Vickers hardness values of unaged Cu alloys show that the alloy with higher Ni content has a slightly higher value but the differences between the three Cu alloys are not significant. However, the three Cu alloys have different tendencies in the changes of hardness with ageing time. In the Cu–4Ni alloy, the hardness values gradually decrease with ageing time and any sign of hardness increase is not detected. On the contrary, in the Cu–5.5Ni and Cu–7Ni alloys, hardness values increase with ageing time, reach peak values after ageing for $10^3$ s, then decrease. Among the two alloys, the Cu–7Ni alloy has a larger increase in hardness with the same ageing time than the Cu–5.5 Ni alloy and the ageing time showing peak hardness value shifts towards a longer period with increased Ni content.

Tensile test results of the equally treated Cu alloys are given in Fig. 2. The trend of tensile strength data is similar to that of hardness data. Ultimate tensile strength of the Cu–4Ni alloy monotonically decreases with ageing time and that of the Cu–5.5Ni and Cu–7Ni alloys increases with ageing time, reaching maximum values at $10^3$ s and decreasing with further ageing.

Elongation increases sharply when microhardness and strength pass the maximum values. The Cu–4Ni alloy shows the highest elongation of the three alloys.

### 3.2. Microstructure characterization

The Cu–7Ni and Cu–4Ni alloys show different tendencies to mechanical property changes during ageing treatments. Therefore, microstructural changes resulting from ageing are characterized for the Cu–4Ni and Cu–7Ni alloys, especially, by X-ray diffractometry and TEM in order to understand the response of different mechanical properties to ageing.

#### *3.2.1. X-ray diffraction analysis*

X-ray diffraction (XRD) analysis shows that no distinct peaks, except those from the Cu matrix, are detected in the samples aged up to $10^3$ s for all specimens. The volume fraction and the size of secondary

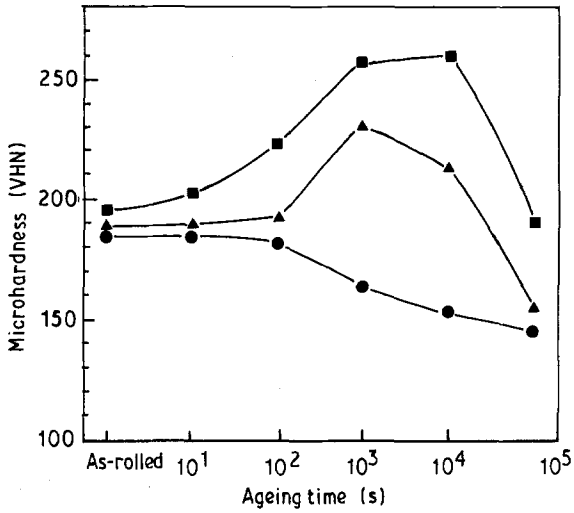


*Figure 1* Microhardness changes during ageing at 500 °C in the Cu–Ni–Al alloys. (●) Cu–3% Al–4.0% Ni; (▲) Cu–3% Al–5.5% Ni, (■) Cu–3% Al–7.0% Ni.

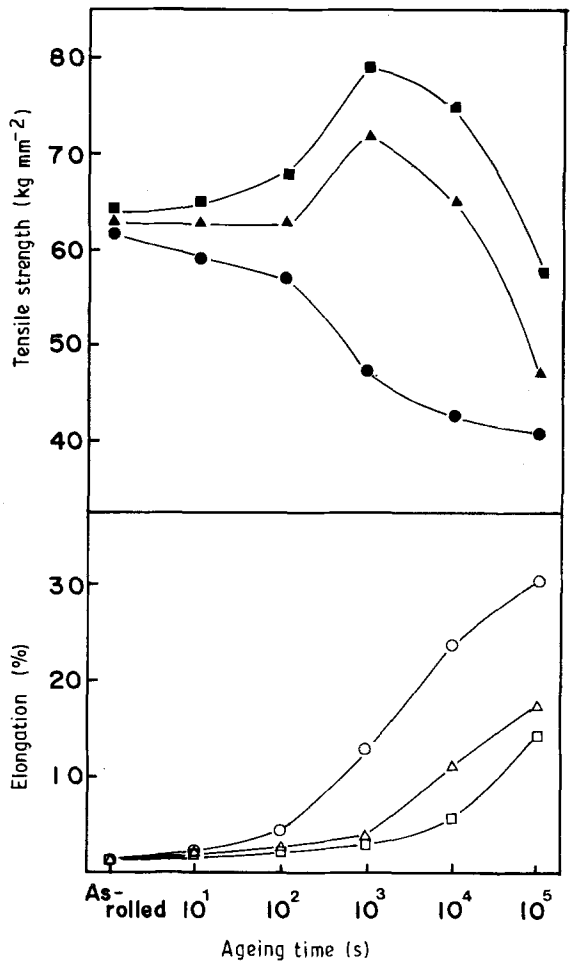


*Figure 2* Changes in (●, ▲, ■) tensile strength and (○, △, □) elongation during ageing at 500 °C in the Cu–Ni–Al alloys. (●, ○) Cu–3% Al–4.0% Ni, (▲, △) Cu–3% Al–5.5% Ni, (■, □) Cu–3% Al–7.0% Ni.

phases may be too small to be detected by XRD. The alloys aged longer reveal secondary peaks. Fig. 3a and b are the XRD patterns of the Cu–4Ni and Cu–7Ni alloys aged for $10^5$ s. The peaks corresponding to (1 0 0) and (1 1 0) of the NiAl phase, and (1 1 0) and (1 1 1) of the $Ni_3Al$ phase are detected in the Cu–7Ni alloy. The (1 1 0) NiAl peak is visible in the Cu–4Ni

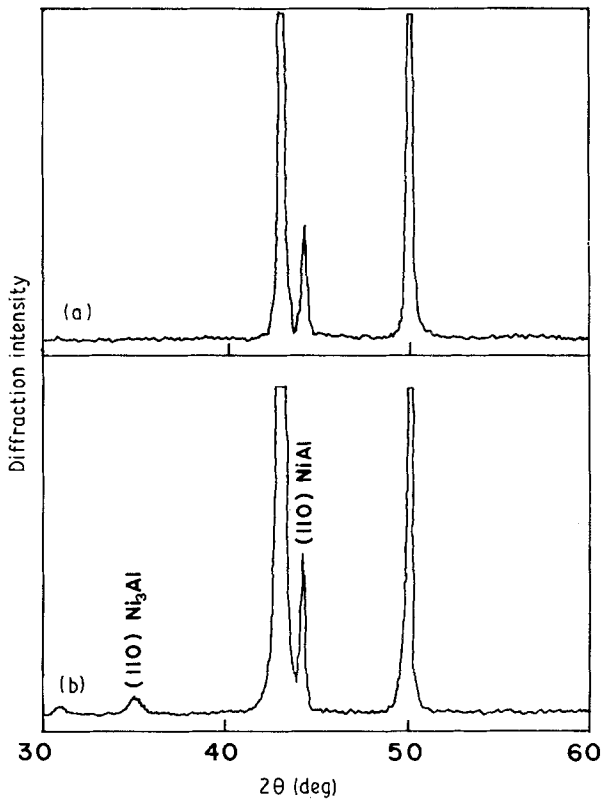


*Figure 3* X-ray diffraction patterns of Cu–Ni–Al alloys aged for $10^5$ s at 500 °C. (a) Cu–4% Ni–3% Al, and (b) Cu–7% Ni–3% Al.

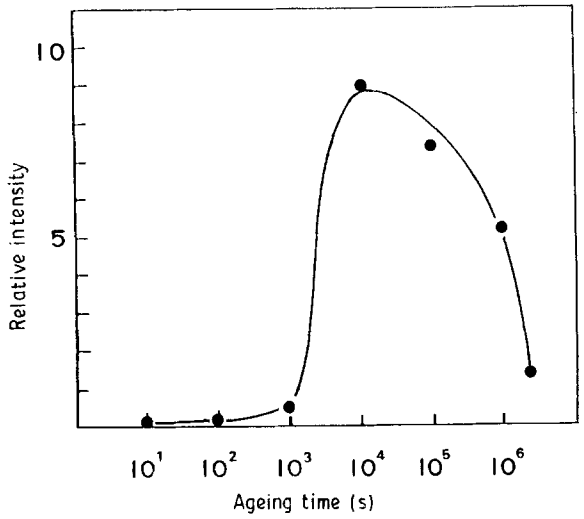


*Figure 4* Changes in volume per cent $Ni_3Al$ in the Cu–7% Ni–3% Al alloy during ageing at 500 °C. The relative intensity of $Ni_3Al$ (1 1 0) is plotted as a function of ageing time.

alloy. The change in the relative volume per cent $Ni_3Al$ in the Cu–7Ni alloy with ageing time up to $2 \times 10^6$ s at 500 °C is shown in Fig. 4. The relative volume per cent $Ni_3Al$ is determined by comparing the (1 1 0) peak intensity of $Ni_3Al$ with that of (2 0 0) of Cu. The relative volume per cent of $Ni_3Al$ is maximum at $10^4$ s and decreases with further ageing, and the $Ni_3Al$ peak almost disappears as the ageing time was increased to $> 10^6$ s.

The above data indicate the presence of $Ni_3Al$ and/or NiAl precipitates in these aged alloys. However, detailed analysis using TEM is necessary to characterize the size, shape, and distribution of the precipitates.

### 3.2.2. TEM analysis of the Cu–7Ni alloy

The microstructure of the Cu–7Ni alloy aged at 500 °C for $10^3$ s is shown in Fig. 5. Dislocation of cell structure due to heavy deformation still remains and recovery is observed in some areas, but no indication of recrystallization is noticeable. Selected-area diffraction and dark-field image reveal the fine precipitates in the Cu matrix (Fig. 6). Attempts were made to identify precipitates by electron diffraction analysis. An indexed diffraction pattern is shown in Fig. 6b. They are


*Figure 5* Transmission electron micrograph of the Cu–7% Ni–3% Al alloy aged at 500 °C for $10^3$ s.

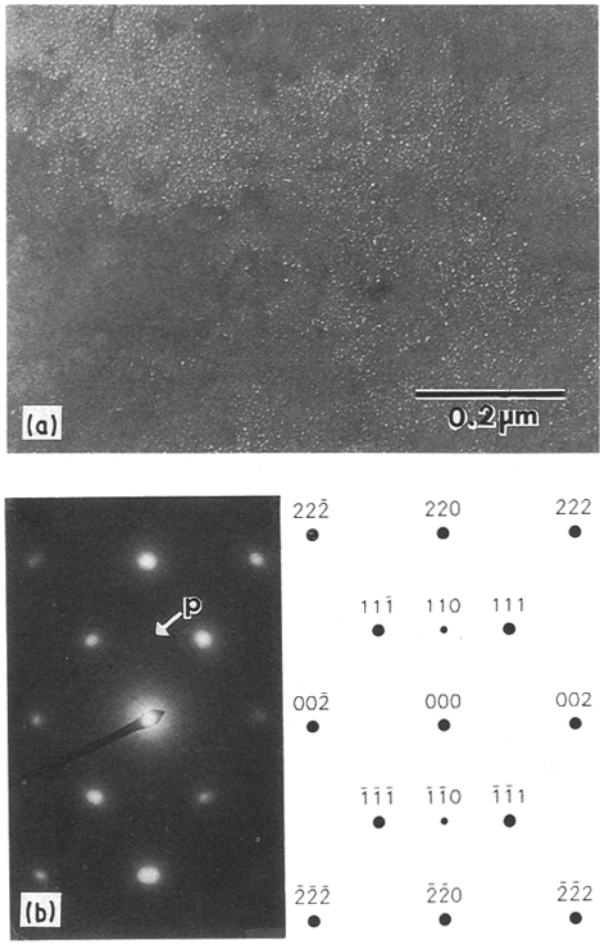


*Figure 6* (a) TEM dark-field image showing $Ni_3Al$ precipitates. (b) Selected-area diffraction pattern in the Cu–7% Ni–3% Al alloy aged at 500 °C for $10^3$ s.

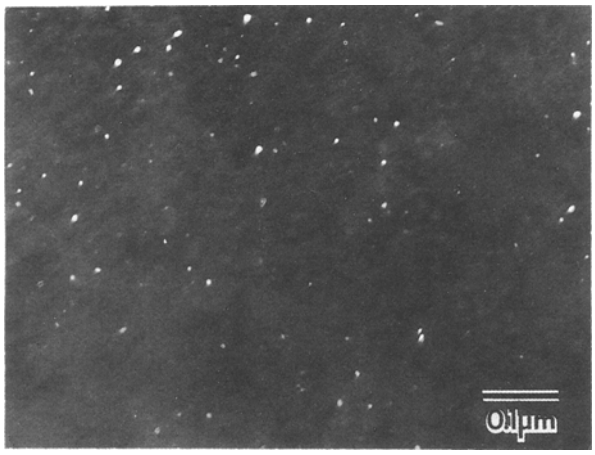


*Figure 7* TEM dark-field image showing $Ni_3Al$ precipitates in the Cu–7% Ni–3% Al alloy aged at 500 °C for $10^4$ s.

identified as $Ni_3Al$ with $L1_2$-type ordered structure [5, 6]. NiAl precipitates are not observed. $Ni_3Al$ precipitates are extremely fine and uniformly distributed. The size of the $Ni_3Al$ precipitates is 2–5 nm at this ageing stage. An orientation relationship between the $Ni_3Al$ precipitate and the Cu matrix exists: $(1\,1\,0)_{Ni_3Al} \parallel (2\,2\,0)_{Cu}$. $Ni_3Al$ particles are spherical and the misfit strain caused by the formation of the precipitates is not large, which is supported by an absence of a streak near the dark-field diffraction spots (Fig. 6) [3].

When the specimen was aged for $10^4$ s, $Ni_3Al$ precipitates were slightly coarsened (Fig. 7). Small recrystallized and dislocation-free grains were sometimes visible. NiAl precipitates were generally seen in the recrystallized grains. The measured size of the $Ni_3Al$ precipitates is about 7 nm and that of the NiAl precipitates is about 200 nm.

When this Cu–7Ni alloy was aged for $10^5$ s, recrystallization proceeds. Relatively large particles and very fine particles are precipitated together, as shown in Fig. 8. Large particles are identified as NiAl phase and fine particles as $Ni_3Al$ phase. The growth and coarsening rate of $Ni_3Al$ particles is apparently very low, but NiAl precipitates becomes larger reaching a size of 350 nm. $Ni_3Al$ particles are distributed uniformly even near the NiAl particles. This phenomenon is different from the observations of Leo and Wassermann [6] where $Ni_3Al$ was depleted near the NiAl particle. The reason for this discrepancy is not clear. It is also noticed in Fig. 8c that $Ni_3Al$ precipitates are preferentially located along the twin boundaries and dislocations.

### 3.2.3. TEM analysis of the Cu–4Ni alloy

Fig. 9 shows the TEM of the Cu–4Ni alloy aged at 500 °C for $10^3$ s. It is noted that the new dislocation-free recrystallized grains nucleate from the heavily deformed region, but cold-worked structure is also present. The precipitates revealed in the dark-field image (Fig. 9b) are identified as NiAl phase. Most of them are present in the recrystallized grains. Also it is interesting that they are selectively observable along the boundary where the recrystallization proceeds (arrows in Fig. 9a,b). These precipitates in the boundary between the recrystallized and unrecrystallized grains are not round, and are relatively small in size.

When the Cu–4% Ni alloy was aged for $10^5$ s, most regions were recrystallized and the precipitates were coarsened to 200–500 nm (Fig. 10). These precipitates are confirmed to be NiAl from the microdiffraction pattern (Fig. 10b). NiAl precipitates found in the Cu–7Ni or Cu–4Ni alloy do not have an orientation relationship with the matrix. $Ni_3Al$ precipitates were not detected under any ageing conditions in the Cu–4Ni alloy.

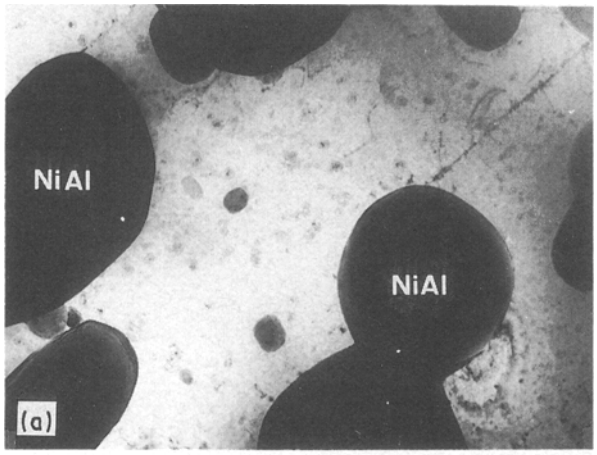


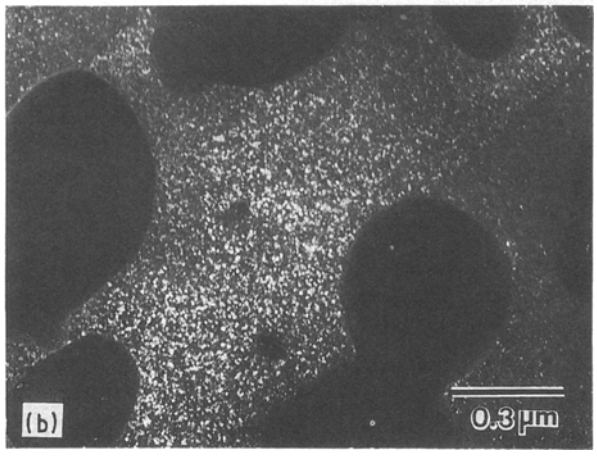


*Figure 8* Transmission electron micrographs of the Cu–7% Ni–3% Al alloy aged at 500 °C for $10^5$ s. (a) Bright-field image, (b) dark-field image showing $Ni_3Al$ precipitates, and (c) bright-field image showing $Ni_3Al$ particles on dislocations and twin boundaries.

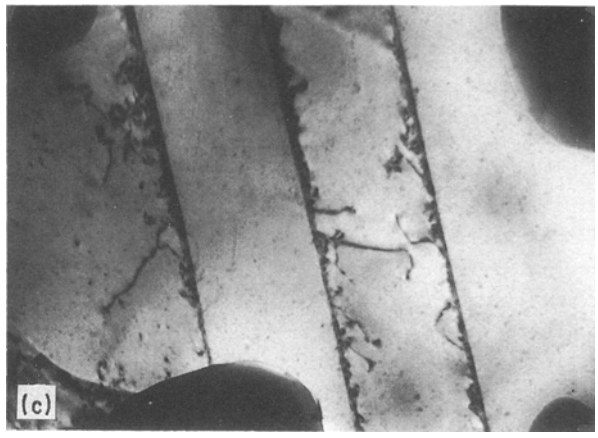

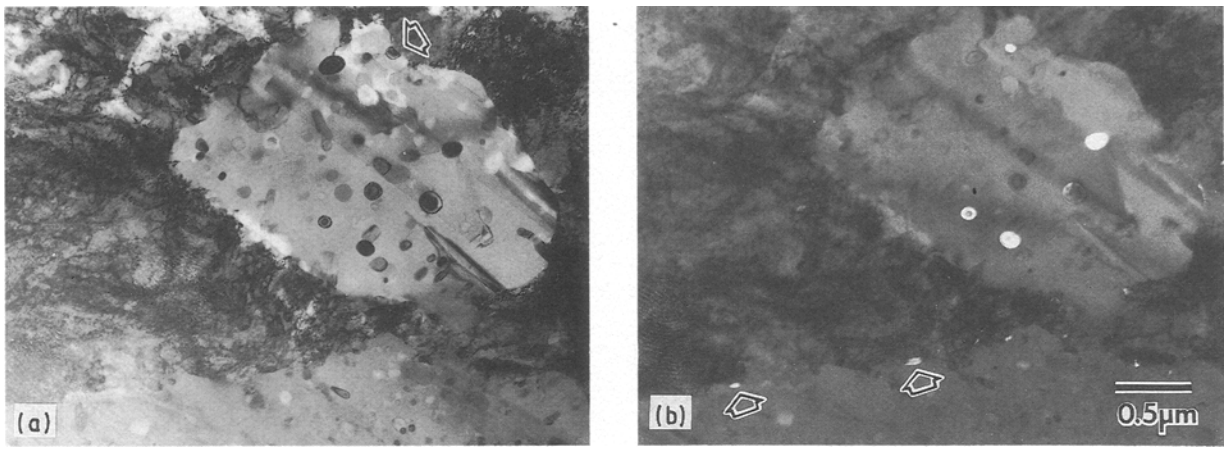


*Figure 9* Transmission electron micrographs of the Cu–4% Ni–3% Al aged at 500 °C for $10^3$ s. (a) Bright-field image, and (b) dark-field image showing NiAl precipitates.

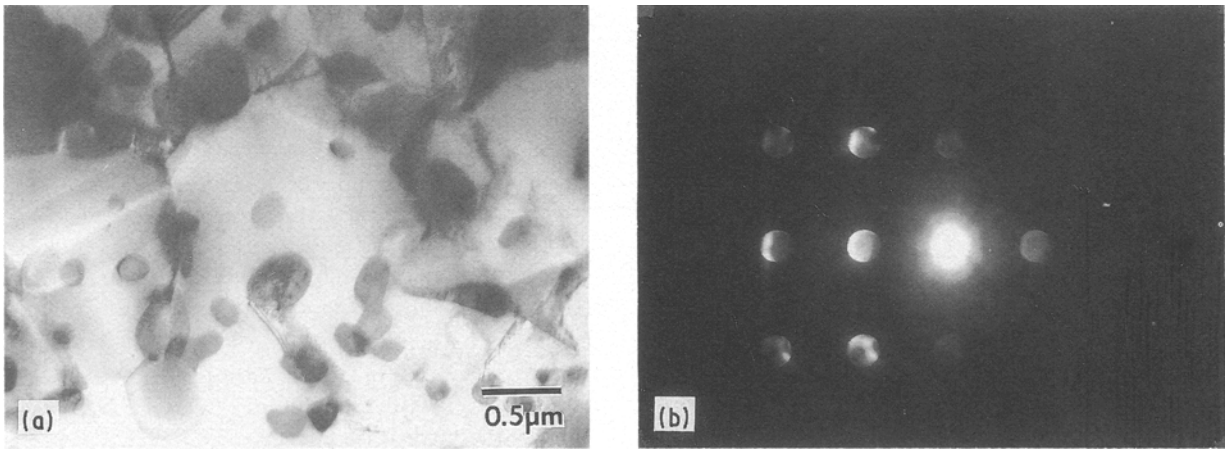


*Figure 10* Transmission electron micrograph and microdiffraction pattern showing an NiAl phase in Cu–4% Ni–3% Al alloy aged at 500 °C for $10^5$ s.

### 3.3. Recrystallization phenomena

In the Cu–7Ni alloy, recrystallized grains were not observed in the specimen aged for $10^3$ s but were seen in the specimen aged for $10^4$ s, which implies that recrystallization started between $10^3$ and $10^4$ s at 500 °C. On the other hand, the fact that recrystallized grains were detected in the Cu–4Ni alloys aged for $10^3$ s indicated recrystallization started before $10^3$ s ageing time. These observed phenomena indicate that the Cu–7Ni alloy has a longer incubation time for recrystallization than the Cu–4Ni alloy, even though the recrystallization start time has not been measured systematically. To confirm this, the three cold-worked Cu alloys were heat treated at 680 °C for 2 h and each microstructure was examined by optical microscopy (Fig. 11). Recrystallization was completed and grain growth proceeded in the Cu–4Ni alloy. However, in case of the Cu–7Ni alloy, an unrecrystallized area was still visible and the overall grain size was very fine. The Cu–5.5Ni alloy shows a degree of recrystallization in between the Cu–4Ni and Cu–7Ni alloys.

Optical microscopic observation of the three Cu alloys aged at 500 °C for $2 \times 10^6$ s revealed similar results, that is, the larger the Ni content, the smaller is the portion of the recrystallized region at the same ageing time. Observations by optical microscopy are consistent with the TEM results, in that recrystallization is retarded in the higher Ni content alloy. Similar phenomena were observed in Cu–Be alloys where the temperature at the onset of recrystallization increases with Be content [9].

### 3.4. Comparison with undeformed and aged Cu–7Ni alloy

The Cu–7Ni alloy was solution treated and aged at 500 °C for $10^4$ s without deformation. The microhardness value of this undeformed alloy is well below that of the deformed alloy in the unaged or in the same aged conditions when compared with Fig. 1, but increases from 82 to 120 VHN due to ageing.

Its microstructure after ageing is shown in Fig. 12. The spherical precipitates revealed in the dark-field image are $Ni_3Al$. The size of these $Ni_3Al$ is about 25 nm. $Ni_3Al$ precipitates maintain a coherency with the matrix and have the same orientation relationship with the Cu matrix as is found in the deformed and aged Cu–7Ni alloy.

The increase in hardness due to ageing in this undeformed alloy is attributed to the coherent $Ni_3Al$ precipitate because strain hardening and recrystallization processes have not been involved. Consequently

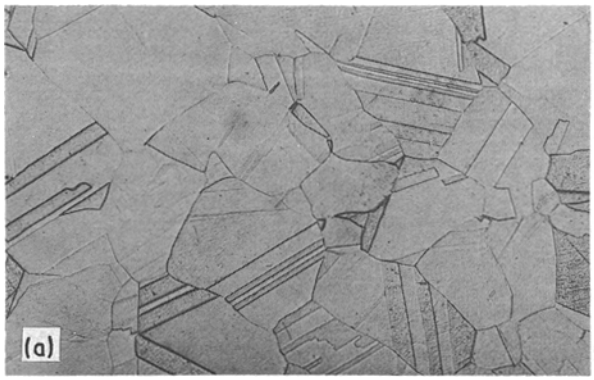



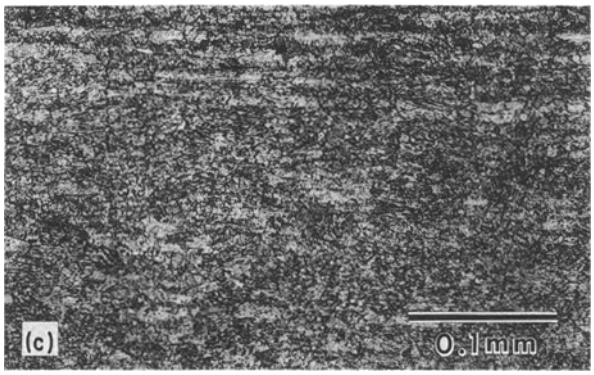


*Figure 11* Optical micrographs of Cu–Ni–Al alloy aged at 680 °C for 2 h. (a) Cu–4% Ni–3% Al, (b) Cu–5.5% Ni–3% Al, (c) Cu–7% Ni–3%Al.

coherent $Ni_3Al$ precipitates have a hardening effect by themselves.

## 4. Discussion

### 4.1. Precipitate formation

Precipitate formation occurs in two different ways depending on Ni content. In the Cu–4Ni alloy, only NiAl phase was formed under the ageing conditions studied here. In the Cu–7Ni alloy, coherent $Ni_3Al$ phase was precipitated in the early stage of ageing and further ageing led to the precipitation of NiAl phase. The appearance of the two different types of precipitation phenomena in these alloys is evidently due to the difference in Ni content in the Cu solid solution.

The ternary phase diagram of the Cu–Ni–Al system at 500 °C (Fig. 13) [10] shows that all three Cu alloys studied here fall in the region of Cu solid solution and NiAl(β) phase at equilibrium. The NiAl phase forms an incoherent interface with the Cu matrix and has a large misfit with respect to the Cu matrix and consequently a high interfacial energy [11]. The energy barrier for nucleation would be large. Thus, when the precipitates are formed from a solid solution supersaturated with Ni and Al, it is energetically favourable for a coherent phase to be precipitated out first because coherent particles have a very low interfacial energy. Calculation of the misfit between $Ni_3Al$ and Cu yields about 1.5%, so relatively little coherency strain is associated with the formation of coherent $Ni_3Al$ precipitates. The formation of spherical coherent particles with a minimum interfacial energy minimizes the nucleation energy.

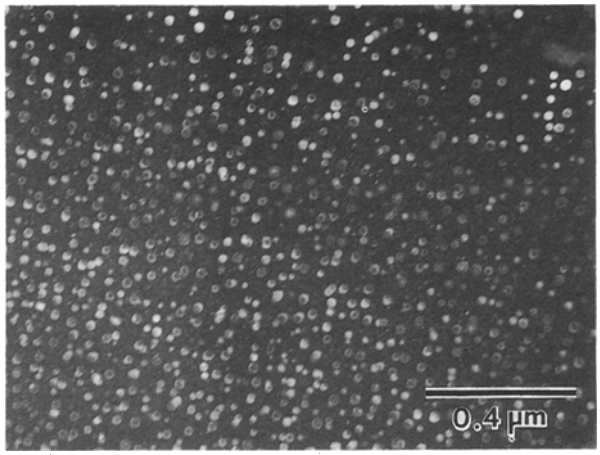


*Figure 12* TEM dark-field image of $Ni_3Al$ precipitates in a Cu–7% Ni–3% Al alloy aged at 500 °C for $10^4$ s without deformation.

The equilibrium phase diagram does not predict the formation of $Ni_3Al$ phase in Cu–3% Al–7% Ni. However, $Ni_3Al$ may form during the initial stage of nucleation to minimize the energy barrier for nucleation. The Cu–3% Al–7% Ni alloy, in particular, approaches the region where solid solution, NiAl, and $Ni_3Al(\kappa)$ phases coexist together (Fig. 13). The possibility of the formation of $Ni_3Al$ from the supersaturated solid solution in the Cu–7Ni alloy is very high due to the local fluctuation of alloying elements. $Ni_3Al$ phase formed at an early stage of ageing in the Cu–7Ni alloy seems a transient phase according to the equilibrium phase diagram and the X-ray diffraction experiment presented earlier (Fig. 4). Fig. 4 clearly shows that the volume fraction of $Ni_3Al$ phase is reduced in the Cu–7Ni alloy aged for $> 10^5$ s. $Ni_3Al$ particles seem to be dissolved when the alloy is aged longer than this. Leo and Wassermann's observation [6] of a Cu–6 wt % Ni–5 wt % Al alloy, of composition similar to those of the present alloys, also suggests that $Ni_3Al$ is not a stable phase because the formation of NiAl caused the depletion of $Ni_3Al$ precipitates near the NiAl particles.

The kinetics of $Ni_3Al$ precipitate formation is closely related to the amount of plastic deformation. When the Cu–7Ni alloy is cold worked more heavily, the maximum value in the hardness–ageing time curve is obtained at shorter ageing times [12]. TEM results imply that the heterogeneous nucleation is dominant in the Cu–7Ni alloy. It is suggested that heterogeneous

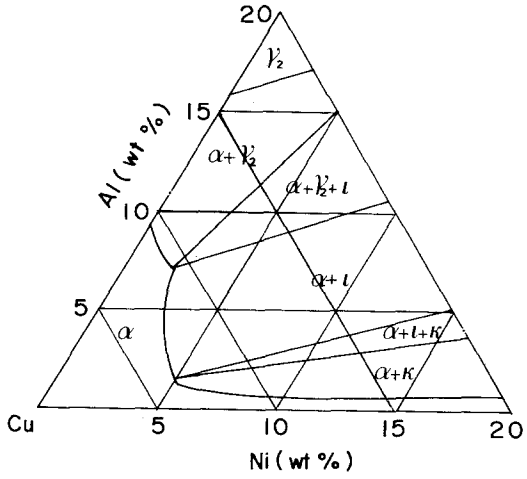


*Figure 13* The 500 °C isotherm for Cu–Ni–Al phase equilibria. The Cu-rich corner is redrawn from [10].

nucleation is favourable if the misfit between precipitate and matrix is larger than 1% [13, 14]. The most favourable sites of precipitate formation are dislocations and boundaries. If nucleation on dislocations or boundaries results in the destruction of defects, some free energy will be released, thereby reducing the activation energy barrier. Nucleation on dislocations or boundaries can be assisted by reducing the total strain energy of the nuclei and by enhancing the diffusion of the solute atoms through a pipe diffusion [11, 14]. An increased amount of deformation and thus increased density of structural defects, such as dislocations and vacancies, which provide nucleation sites, intensify precipitation. Therefore, $Ni_3Al$ precipitates are very fine in the heavily deformed structure (Figs 6, 7) and relatively coarse in the undeformed structure (Fig. 12).

It is not clear in the Cu–4Ni alloy whether an undetectable amount of $Ni_3Al$ phase was formed before the NiAl phase precipitated out. However, differential thermal analysis (DTA) showed that only one peak was detected in the Cu–4Ni alloy during ageing, supporting the fact that $Ni_3Al$ particles are not likely to form [12]. It is shown in Fig. 9 that some NiAl precipitates are located in the recrystallization front and they are relatively small and not spherical. These phenomena imply that the boundary between the recrystallized and unrecrystallized grains may offer a nucleation site for NiAl precipitates, because the recrystallization front plays a role in the active diffusion path and nucleation in the boundaries may reduce the energy barrier for nucleation.

### 4.2. Effects of microstructure on mechanical properties

Ageing of a heavily deformed supersaturated Cu solid solution involves two opposite processes:

(a) softening due to recovery and recrystallization by elimination of the deformation distortions in the structure;

(b) hardening due to precipitates formed from the supersaturated solid solution.

The hardness value in the Cu–7Ni alloy increases with ageing time up to $10^4$ s and ageing process produces a fine distribution of extremely small coherent $Ni_3Al$ precipitates. The $Ni_3Al$ particles at the point of maximum strength are extremely small, about 2–5 nm. Hardness increases due to ageing in the undeformed Cu–7Ni alloy, and hardness decreases due to ageing in the deformed Cu–4Ni alloy, clearly prove that coherent $Ni_3Al$ particles are a source of strengthening. These coherent particles are relatively powerful in increasing the strength, according to Tsuda *et al.* [7]. The main strengthening mechanisms suggested by these authors are the interaction of dislocations with the strain field of coherent precipitates, and the cutting of ordered precipitates by superlattice dislocations. The strength can be increased further by a higher precipitate density, resulting from a heavy deformation [12].

Another interesting point is that these coherent particles slow the recrystallization process. Coherent $Ni_3Al$ precipitates are formed before recrystallization begins in the Cu–7Ni alloy. Coherent precipitates can retard or stop the movement of dislocations and boundaries, because this behaviour reduces the elastic energy of dislocations [9]. The above explanation is confirmed by the presence of precipitates on dislocations and boundaries. Another reason may be that a moving dislocation has difficulty in cutting through coherent precipitates [9]. It is well known that recovery and recrystallization accompany not only rearrangement and annihilation of dislocations, but also boundary movement and cell growth. In consequence, the recrystallization process will be delayed in the Cu–7Ni alloy where coherent particles have already been precipitated. Similar phenomena seem to operate in the Al–Cu [9] and Ni–Al alloys [15]. When precipitates in these alloys are of a coherent nature, the activation energy of recrystallization increased 1.5–2 times and the rate of the recrystallization process decreased by two or more orders of magnitude.

On the other hand, hardness gradually decreases as ageing time increases in the Cu–4Ni alloy where only NiAl particles are detected. The decrease in hardness is attributed to the recrystallization accompanying a reduction of the strain-hardening effect. NiAl precipitates form with ageing, but these particles are not effective in compensating the decrease in strength due to recrystallization, because they are an incoherent phase and coarsen rapidly.

## 5. Conclusion

Cu alloys containing 5.5% and 7% Ni show that microhardness and tensile strength increase with ageing time and reach maximum values at ageing times of $10^3$–$10^4$ s, then decrease. Meanwhile, in a Cu alloy containing 4% Ni, microhardness and tensile strength decrease gradually with increasing ageing time. The $Ni_3Al$ phase is first precipitated out during the early stage of ageing and later NiAl phase is precipitated in Cu–7% Ni–3% Al alloy, but only NiAl phase is formed in Cu–4% Ni–3% Al alloy. Very fine $Ni_3Al$ particles formed in the 7% Ni alloy are coherent with the matrix and did not coarsen much. The volume fraction of $Ni_3Al$ particles, however, decreased

after ageing for $10^6$ s and this seems to indicate that $Ni_3Al$ particles are dissolved when aged for a long time. NiAl particles are incoherent with the matrix and most NiAl particles are located in the recrystallized grains. Recrystallization starts earlier in the 4% Ni alloy than in the 7% Ni alloy. Conclusively, in the 7% Ni alloy, formation of fine coherent $Ni_3Al$ particles results in precipitation hardening. Moreover, the strain-hardening effect is not diminished by the role of $Ni_3Al$ retarding the recrystallization process. In the 4% Ni alloy, incoherent NiAl phase is not effective in increasing the strength, therefore the strength decreases due to the recrystallization process during the ageing treatment.

## References


1. W. BONFIELD and B. C. EDWARDS, *J. Mater. Sci.* **9** (1974) 398.
2. *Idem., Ibid.* **9** (1974) 415.
3. R. KNIGHTS and P. WILKES, *Acta Metall.* **21** (1973) 1503.
4. J. M. POPPLEWELL and J. CRANE, *Metall. Trans.* **2** (1971) 3411.
5. H. BOHM and W. LEO, *Harterei-Techn. Mitteilungen* **19** (1964) 79.
6. W. LEO and G. WASSERMANN, *Metall.* **21** (1967) 10.
7. H. TSUDA, T. ITO and Y. NAKAYAMA, *J. Jpn. Inst. Metal.* **44** (1980) 431.
8. K. E. AMIN and P. C. BECKER, *Mater. Sci. Engng* **49** (1981) 173.
9. S. S. GORELIK, in "Recrystallization in Metals and Alloys" (Mir, Moscow, 1981) pp. 379–413.
10. Metals Handbook, 8th Edn, Vol. 8 (ASM, Metals Park, 1973) pp. 388–9.
11. D. A. PORTER and K. E. EASTERLING, in "Phase Transformation in Metals and Alloys" (Van Nostrand Reinhold, New York, 1981) pp. 142–64, 263–78.
12. Y. R. CHO, MS thesis, KAIST, Korea (1986).
13. H. WARLIMONT, in "Electron Microscopy and Structure of Materials", Proceedings of the 5th International Materials Symposium, edited by G. Thomas (University of California Press, Berkeley, 1972) pp. 505–37.
14. S. SHAPIRO, D. E. TYLER and R. LANAM, *Metall. Trans.* **5** (1974) 2457.
15. H. KREYE, E. HORNBOGEN and F. HAESSNER, *Phys. Status Solidi (a)* **1** (1970) 97.



*Received 7 November 1989*
*and accepted 6 March 1990*